Antiferromagnetism in the Face-Centered Cubic Lattice. II. Magnetic Properties of MnO

M. E. LINES* AND E. D. JONES†
Bell Telephone Laboratories, Murray Hill, New Jersey
(Received 29 March 1965)

The somewhat anomalous properties of MnO have recently been cited as evidence for the existence of significant biquadratic exchange in this salt. The present paper suggests that this conclusion is not justified and that the magnetic properties of MnO can be quantitatively explained in the complete absence of biquadratic exchange. MnO is a face-centered cubic antiferromagnet. The anomalous properties are shown to result from the sensitivity of bilinear exchange to inter-ion distance, which results (for MnO) in an anisotropic distortion of the cubic lattice for temperatures below the Néel point T_N. The random-phase Green's function theory of Part I is used to describe the magnetic susceptibility for $T>T_N$, and to investigate the sublattice magnetization as a function of temperature for $T<T_N$. Good agreement between theory and experiment is obtained, and values $J_1=10°K$ and $J_2=11°K$ are calculated for the nearest-neighbor and next-nearest-neighbor exchange parameters, respectively. The molecular-field theory is shown to be far too crude an approximation to give quantitatively satisfactory results. The Mn^{55} zero-field nuclear magnetic resonance (NMR) has been observed in the antiferromagnetic state of MnO and, from the temperature dependence of the resonance frequency, information regarding the spin deviation as a function of temperature is derived. A simple noninteracting spin-wave theory has been developed to describe the spin deviation, and a satisfactory description of the low-temperature properties is obtained. A calculation is also presented for the contribution of the indirect nuclear spin-spin interaction to the NMR linewidth.

1. INTRODUCTION

THE magnetic properties of the antiferromagnet MnO are currently of considerable interest because it has been suggested[1] that they present evidence for the existence of intrinsic biquadratic exchange in ordered magnetic systems. Theoretically, the superexchange mechanism is expected to give rise to terms of the form $j(\mathbf{S}_1\cdot\mathbf{S}_2)^2$ in addition to the usual Heisenberg bilinear exchange,[2] but these biquadratic effects occur in a high order of a fairly rapidly converging perturbation theory, and are therefore small and difficult to calculate with any accuracy. First efforts towards a quantitative evaluation of j have recently been made by Huang and Orbach,[3] who find that it may well be large enough to produce observable effects in MnO.

The situation is complicated, however, by the fact that effective biquadratic terms can also arise via a mechanism in which a balance is set up between exchange and elastic forces.[4–6] The question arises, therefore, as to which effect is predominantly responsible for the anomalous magnetic properties of MnO. This question has been further complicated by a recent calculation by Harris,[7] which suggests that some of the anomalies, at least, may be explained without recourse to either of the above mechanisms, but merely by treating the bilinear exchange Hamiltonian in a sufficiently accurate statistical approximation.

In the present paper, we use Green's function and spin-wave techniques to examine in detail the magnetic properties of MnO. We find that the so called anomalous properties may be understood by studying the effects of exchange-induced distortion of the cubic lattice structure,[6] and that a quantitative agreement between theory and experiment may be obtained by use of the above statistical theories. The molecular-field theory would seem to be far too crude and approximation to give quantitatively satisfactory results. We are in disagreement with Harris,[7] finding that the magnetic properties cannot be explained if exchange-induced crystal distortion is ignored (see Part I). They may be quantitatively explained, however, without any need to invoke superexchange biquadratic terms and therefore they do not present evidence for the existence of such terms. On the other hand, we are not able to show that biquadratic interactions are necessarily entirely absent, because the most significant anomalous property (the shape of the magnetization curve) is rather insensitive to the presence of a small biquadratic term in addition to the observed magnetostriction.

The large effects of exchange-induced distortion in MnO result from a rather unusual property of the antiferromagnetic spin pattern found in this salt. Similar effects may be expected to occur in other salts which exhibit this same spin structure (e.g., NiO, α-MnS) but such effects can be expected to be a comparative rarity in antiferromagnetism as a whole.

MnO is a face-centered cubic (fcc) antiferromagnet with the rocksalt crystal structure. Early neutron

* Present address: Clarendon Laboratory, Oxford University, Oxford, England.
† Present address: Sandia Laboratory, Albuquerque, New Mexico.

[1] D. S. Rodbell, I. S. Jacobs, J. Owen, and E. A. Harris, Phys. Rev. Letters **11**, 10 (1963)
[2] P. W. Anderson, Phys. Rev. **115**, 2 (1959); in *Magnetism*, edited by G. Rado and H. Suhl (Academic Press Inc., New York, 1963), Vol. 1.
[3] N. L. Huang and R. Orbach, Phys. Rev. Letters **12**, 275 (1964).
[4] C. Kittel, Phys. Rev. **120**, 335 (1960).
[5] C. P. Bean and D. S. Rodbell, Phys. Rev. **126**, 104 (1962).
[6] D. S. Rodbell and J. Owen, J. Appl. Phys. **35**, 1002 (1964).
[7] E. A. Harris, Phys. Rev. Letters **13**, 158 (1964).

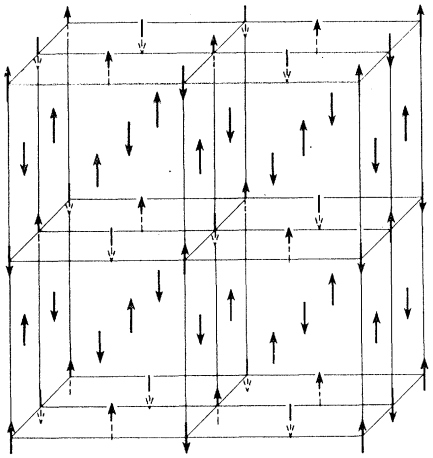

FIG. 1. The type-2 antiferromagnetic spin arrangement in the fcc lattice. In MnO, the axis of spin alignment is contained in the [111] plane.

diffraction experiments[8] gave evidence that the spin ordering was of the second kind[9] (Fig. 1), with all next-nearest neighbors showing an antiparallel correlation, but questions remained for many years as to the preferred direction of spin alignment with respect to the crystal axes and to the possibility of a multiaxis spin structure.[10,11]

In MnO, the ionic configuration $Mn^{++}O^{--}$ should predominate (although recent susceptibility experiments[12,13] indicate that this may not be the case for temperatures much above 300°K), so that the manganese ions are predominantly in S states. For such a case, anisotropy will, in general, be small and arise dominantly from magnetic dipolar interactions. For MnO, the resulting anisotropy energy amounts at most to only a few percent of the isotropic exchange energy. For the fcc ordering of the second kind, Kaplan[14] has shown that the dipolar interactions restrict the spins to lie in the ferromagnetic [111] planes. Keffer and O'Sullivan[10] and Roth[11] point out that this is only true if one disregards the possibility of multiaxial spin patterns. They suggest, however, that the single-axis structure is probably stabilized by the small rhombohedral distortion of the lattice[15] which occurs for temperatures below the Néel point T_N. More recently, Nagamiya[16] has shown that this distortion does, indeed, stabilize the single-axis structure, and there can now be little doubt that the spins in MnO are confined in [111] planes. A very similar situation occurs for NiO where the existence of a single-axis spin structure has now been confirmed experimentally.[17]

The spin structure of MnO is, therefore, as shown in Fig. 1 except that the direction of the single axis of spin alignment should be contained in the [111] plane (a situation which is very difficult to illustrate diagramatically). The spins are not confined to any particular direction within the plane until further anisotropy terms are introduced. Possible sources of such an in-plane anisotropy are discussed by Keffer and O'Sullivan,[10] who indicate that they are likely to be considerably smaller than the dipolar anisotropy.

For temperatures above T_N, MnO has a cubic structure and we shall describe it by the Hamiltonian

$$\mathcal{H}=\sum_{\text{nn}} J_1\mathbf{S}_i\cdot\mathbf{S}_j+\sum_{\text{nnn}} J_2\mathbf{S}_i\cdot\mathbf{S}_j, \qquad (1.1)$$

where $\sum_{\text{nn}}$ and $\sum_{\text{nnn}}$ run over all pairs of nearest and next-nearest neighbors, respectively. We assume that all exchange interactions more remote than these are negligible. For temperatures below T_N we shall include the contributions to the spin Hamiltonian which result from crystal distortion. The importance of such contributions for MnO were noted by Kanamori,[18] and have been discussed more recently by Rodbell and Owen[6] who use a molecular-field theory.

Since bilinear exchange is, in general, separation dependent, most dominantly isotropic magnetic systems will undergo an isotropic contraction when long-range magnetic order sets in. This contraction decreases the free energy by lowering the exchange energy by more than it increases the elastic strain energy. For MnO, however, the effect is small and does not significantly modify the magnetic properties of the system.[19]

The unusual feature of the fcc type-2 spin pattern, which allows for a very much larger effect in MnO, concerns the relative orientation of the nearest-neighbor spins. There are six parallel and six antiparallel nearest neighbors of any particular spin. The six parallel neighbors are all contained in the same [111] plane, and the six antiparallel neighbors are all out of this plane. If we consider possible *anisotropic* deformations of the cubic structure, it is immediately evident that such a system gains exchange energy from a contraction along the (111) body diagonal. For MnO, the balance between exchange and elastic forces occurs when the distorted cube corner angles are $\frac{1}{2}\pi\pm\Delta$, where[20] $\Delta=1.1\times10^{-2}$ at the absolute zero of temperature.

The accompanying magnetic effects are described to a good approximation (see Sec. 3) by introducing, for temperatures below T_N, two nearest-neighbor bilinear

[8] C. G. Shull, W. A. Strausser, and E. O. Wollan, Phys. Rev. **83**, 333 (1951).
[9] P. W. Anderson, Phys. Rev. **79**, 705 (1950).
[10] F. Keffer and W. O'Sullivan, Phys. Rev. **108**, 637 (1957).
[11] W. L. Roth, Phys. Rev. **110**, 1333 (1958); **111**, 772 (1958).
[12] J. J. Banewicz, R. F. Heidelberg, and A. H. Luxem, J. Phys. Chem. **65**, 615 (1961).
[13] J. A. Poulis, C. H. Massen, and P. Van der Leeden, J. Phys. Soc. Japan, **17**, Suppl. B-I, 212 (1962).
[14] J. I.Kaplan, J. Chem. Phys. **22**, 1709 (1954).
[15] N. C. Tombs and H. P. Rooksby, Nature **165**, 442 (1950).
[16] T. Nagamiya, in The Second Welch Foundation Conference, Houston, December 1958 (unpublished).
[17] W. L. Roth and G. A. Slack, J. Appl. Phys. **31**, 352S (1960).
[18] J. Kanamori, Progr. Theoret. Phys. (Kyoto) **17**, 197 (1957).
[19] A. J. Sievers, III, and M. Tinkham, Phys. Rev. **129**, 1566 (1963).
[20] D. S. Rodbell, L. M. Osika, and P. E. Lawrence, J. Appl. Phys. **36**, 666 (1965).

exchange parameters $J_1^{\pm}=J_1\pm 0.10k(\bar{S})^2$, where $\bar{S}$ is the average spin per site, where k is the Boltzmann constant, and where the larger exchange is to be associated with the antiparallel neighbors. For large spin values and low temperatures, these effects are very similar to those which would result from the presence of biquadratic exchange in the system. In general, however, this is not the case (e.g., for $T>T_N$, the distortion effect is completely inoperative whereas a true biquadratic exchange would still be effective) and biquadratic contributions to the Hamiltonian are much more difficult to treat in a satisfactory approximation than are the distortion terms.

Because of this situation, we have attempted to describe the magnetic properties of MnO without introducing real biquadratic exchange. Our main result is that a quantitative agreement between theory and those experimental results which are presently available can be obtained in this way.

In Sec. 2 we discuss the properties of the paramagnetic state using Eq. (1.1), and we evaluate J_1 and J_2 using Green's function theory. We find $J_1=10°$K and $J_2=11°$K. The antiferromagnetic state is considered in Sec. 3, where we discuss the origin of the crystal distortion and its effect on the spin Hamiltonian, and then evaluate the sublattice magnetization as a function of temperature. The latter calculation is carried out by molecular-field and Green's function techniques and the results compared. We find that the molecular-field theory seriously underestimates the effects of the lattice distortion on sublattice magnetization, but that the Green's function theory indicates an agreement between the observed magnitude of the crystal distortion and the shape of the magnetization curves as measured by neutron diffraction experiments.[8]

In Sec. 4, we calculate the temperature dependence of sublattice magnetization at very low temperatures using a simple noninteracting spin-wave approximation. Section 5 describes the experimental observation of Mn^{55} zero-field nuclear magnetic resonance in antiferromagnetic MnO, and discusses the interpretation of the temperature variation of this frequency in terms of the spin-wave calculations of Sec. 4. Also discussed is the resonance linewidth and its dependence on the small "in-plane" anisotropy. Finally, Sec. 6 considers the paramagnetic state in more detail. We find that there can be no anisotropic distortion of the lattice in the absence of long-range order, and discuss the significance of this result when one considers the two-spin correlation functions in the paramagnetic state.

2. THE PARAMAGNETIC STATE

For temperatures above the Néel point, we describe the magnetic properties of MnO using Hamiltonian (1.1). Anisotropy in this temperature region is certainly negligible as long as the $Mn^{++}O^{--}$ description of the system is valid. Let us first consider the transition temperature itself, which is 117±1°K.[21-22]

Theoretical estimates for magnetic-transition temperatures in terms of bilinear-exchange parameters are usually no better than semiquantitative, particularly so for the more complex antiferromagnetic orders of which Fig. 1 is a good example. Perhaps the best estimates presently available for these complicated spin structures are those obtained from Green's function theories. Such a calculation has been carried out for the fcc type-2 order by Lines[23] using the random-phase Green's function approximation. However, there is reason to believe that, for spin $\frac{5}{2}$ (which is the case applicable to MnO), these results are likely to be a little low. The only systems for which the transition temperatures are known with good accuracy are the simple cubic, body-centered cubic, and face-centered cubic ferromagnets with nearest-neighbor exchange only.[24,25] For these cases and spin $\frac{5}{2}$, the random-phase Green's function approximation is, respectively, about 7, 5, and 5% too low. Noting that the discrepancy is largest for the least stable (smallest value of kT_c/J) system, and that the situation for MnO will be less stable than any of these, we shall suppose that the best theoretical estimates for T_N in the fcc type-2 order, are values about 10% above the random-phase Green's function results. These values are shown graphically in Fig. 2.

There are very many published measurements of magnetic susceptibility in MnO for temperatures above

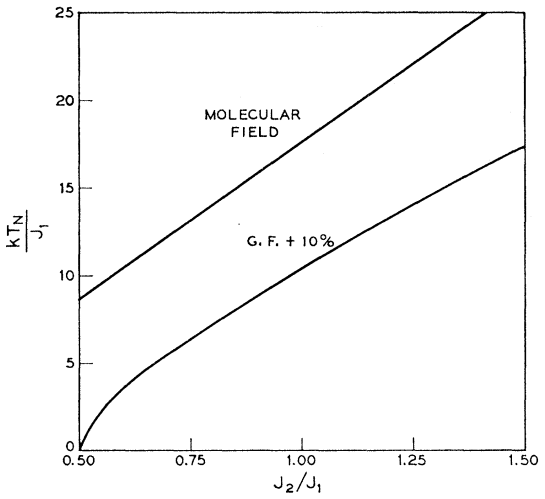

FIG. 2. Theoretical estimates of Néel temperature for the fcc type-2 antiferromagnetic order plotted as a function of the ratio of next-nearest-neighbor to nearest-neighbor exchange (see text).

[21] R. W. Millar, J. Am. Chem. Soc. **50**, 1875 (1928).
[22] S. S. Todd and K. R. Bonnickson, J. Am. Chem. Soc. 73, 3894 (1951).
[23] M. E. Lines, Phys. Rev. **135**, A1336 (1964).
[24] G. S. Rushbrooke and P. J. Wood, Mol. Phys. **1**, 257 (1958).
[25] R. A. Tahir-Kheli, Phys. Rev. **132**, 689 (1963).

the Néel point.[12,13,26–31] They are by no means in quantitative agreement, although there now seems to be little doubt[12,13] that, for temperatures $T \gg T_N$, the susceptibility cannot be described by a function $C/(T+\theta)$, where C is the Curie constant for spin $\frac{5}{2}$. At such temperatures ($5T_N < T < 10T_N$), short-range-order effects are small and the system should be described to quite a good approximation by the molecular-field theory. Experiment shows, however, that the measured value of C is up to 15% below the spin $\frac{5}{2}$ value. The most likely explanation lies with the thermal excitation of the following reactions, in which the electronic states represented are separated by large distances in the crystal:

$$O^{--}(2p^6)+Mn^{++}(3d^5) \rightarrow O^{-}(2p^5)+Mn^{+}(3d^6), \quad (2.1)$$

$$Mn^{++}(3d^5)+Mn^{++}(3d^5) \rightarrow Mn^{+}(3d^6)+Mn^{+++}(3d^4). \quad (2.2)$$

Whatever the reasons, the fact that the Curie constant is so markedly reduced from the spin-$\frac{5}{2}$ value means that no reliance can be attached to any simple interpretation of the associated Curie-Weiss constant θ. Thus, no information concerning J_1 and J_2 is easily obtainable from this very high-temperature data.

For temperatures in the range $T_N \rightarrow 2T_N$, accurate susceptibility measurements have been made by Lindsay[32] (Fig. 3). In this comparatively low-temperature region, we shall suppose[13] that the MnO system may still be described in terms of $Mn^{++}O^{--}$. If so, we can fit the experimental data to the Green's function theory of Part I. This is done in Figs. 3 and 4. The "best fit" determines closely the value of the Curie-Weiss constant as

$$\theta = (12J_1+6J_2)S(S+1)/3k = 540°K, \quad (2.3)$$

and also suggests that the ratio J_2/J_1 is not far removed from unity. Equation (2.3) reduces to $2J_1+J_2=30.9°K$. It is interesting to note that the Green's function theory allows us to extract two pieces of information about the exchange parameters from the paramagnetic susceptibility where a molecular-field theory would give only one.

We may now plot the reduced susceptibility $\chi/\chi(T_N)$ against T/T_N, again comparing the Green's function results of Part I with Lindsay's data. The results are shown in Fig. 5. For temperatures $T_N < T < 2T_N$, the experimental values fall close to the curves $J_2/J_1=1.2$ and 1.3. Using Lindsay's estimated relative accuracy ($\sim 1\%$), we estimate $1.1 < J_2/J_1 < 1.5$. For higher temperatures, the experimental results of Refs. 12, 27, and 30 fall close to the curve $J_2/J_1=1.5$. Allowing, very roughly, for a Curie constant reduction of 10 to 15% at very high temperatures, the ratio $J_2/J_1=1.1$ would seem to be more likely than the value 1.5.

Measurements of magnetic susceptibility *at* the Néel point are reported in Refs. 1, 27, 28, and 30. Values range from 79 to 84, in units of 10^{-6} emu/g. McGuire and Happel[28] measure the susceptibility as a function of magnetic field, whereas most of the other measurements are reported for a single arbitrary value of field, and their results suggest that the lower values are more likely to apply to the zero-field limit. Theoreti-

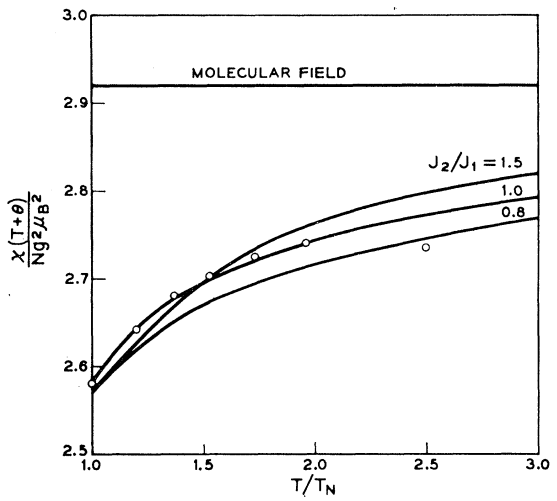

FIG. 3. Curves of magnetic susceptibility, calculated in the random-phase Green's function approximation for spin $\frac{5}{2}$, plotted as a function of temperature and compared with the experimental data of Lindsay (Ref. 32) for the case $\theta=540°K$. (θ is the Curie-Weiss constant).

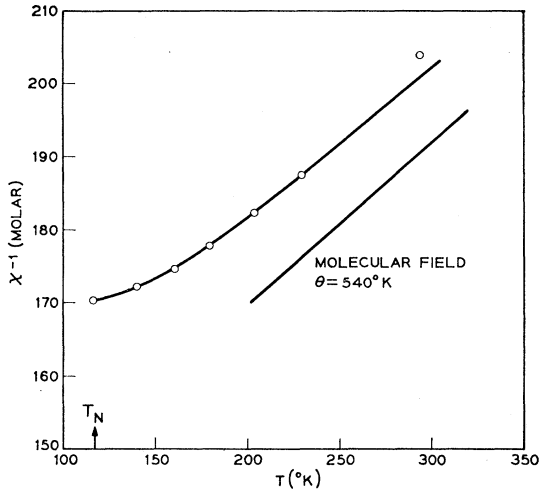

FIG. 4. The curve $J_2/J_1=1.0$ of Fig. 3 replotted by putting $T_N=117°K$ and again compared with Lindsay's data.

[26] H. Bizette, B. Squire, and B. Tsai, Compt. Rend. **207**, 449 (1938).
[27] W. D. Johnston and R. R. Heikes, J. Am. Chem. Soc. **78**, 3255 (1956).
[28] T. R. McGuire and R. J. Happel Jr., J. Phys. Radium **20**, 424 (1959).
[29] S. S. Bhatnager, A. Cameron, E. H. Harbard, P. L. Kapur, A. King, and B. Prakash, J. Chem. Soc. **11**, 1433 (1939).
[30] H. Bizette and B. Tsai, Compt. Rend. **217**, 444 (1943).
[31] R. W. Tyler, Phys. Rev. **44**, 776 (1933).
[32] R. Lindsay (unpublished).

cally, the zero field magnetic susceptibility at T_N may be written,[23] in standard notation,

$$\chi(T_N)=Ng^2\mu_B^2/12(J_1+J_2), \quad (2.4)$$

where the molecular-field theory and the random-phase Green's-function theory give the same result. Equating this expression to 80×10^{-6} emu/g, gives $J_1+J_2=22.1°$K.

A check on this value for J_1+J_2 can be obtained from the perpendicular susceptibility at absolute zero. The only direct measurement of this quantity presently available is that of Rodbell *et al.*,[1] who give $\chi_\perp(T=0)$ equal to $(74\pm5)10^{-6}$ emu/g. Theoretically, the best expression for low-temperature perpendicular susceptibility is that obtained from spin-wave[33] or Green's function[23] theories. For MnO it may be written

$$\chi_\perp(T=0)=Ng^2\mu_B^2/[12J_1^+(1+\Delta_{nn}) +12J_2(1+\Delta_{nnn})], \quad (2.5)$$

where $J_1^+=J_1+0.10k(\bar{S})^2$, as described in Sec. 1 (see also Sec. 3), and where Δ_{nn} and Δ_{nnn} refer respectively to antiparallel nearest and next-nearest neighbors i and j, where

$$\Delta=\langle S_{ix}S_{jx}\rangle/(\bar{S})^2. \quad (2.6)$$

In this expression, x is a direction perpendicular to the spin alignment, and the angular brackets represent an ensemble average. The effects represented by Δ_{nn} and Δ_{nnn} are quite small and for our purpose it will be sufficient to write $\Delta_{nn}=\Delta_{nnn}=\Delta$. For the simple cubic antiferromagnet $\Delta=0.13/\bar{S}$, or, for spin $\frac{5}{2}$, $\Delta\approx0.05$. For MnO, the value is likely to be a little smaller, because the zero-point spin-wave deviations are smaller for MnO (see Sec. 4) than they are for the isotropic simple cubic case. We shall take values $\Delta\approx0.04$, and $J_1^+-J_1\approx0.6°$K, when we find

$$\chi_\perp(T=0)=Ng^2\mu_B^2/(12J_1^+ +12J_2)1.04 =(74\pm5)10^{-6} \text{ emu/g}. \quad (2.7)$$

and the result $J_1+J_2=22.4\pm1.5°$K.

We may now combine the above results to see whether they are consistent within the available theories and, if so, to estimate the values of J_1 and J_2 which exist in MnO. Within the range $0.8<J_2/J_1<1.5$, the condition that T_N is 117°K and is given by Fig. 2 may be written, to a good approximation, as

$$J_2-0.3J_1=8.0°\text{K}. \quad (2.8)$$

We may summarize our findings as follows:

$$\begin{aligned}&\text{(i)}\quad \text{from } \chi(T>T_N); && 2J_1+J_2=30.9°\text{K},\\ &\text{(ii)}\quad \text{from } \chi(T_N); && J_1+J_2=22.1°\text{K},\\ &\text{(iii)}\quad \text{from } T_N; && J_2-0.3J_1=8.0°\text{K},\\ &\text{(iv)}\quad \text{from } \chi(T>T_N); && J_2/J_1=1.25\pm0.25.\end{aligned} \quad (2.9)$$

The first three results should not be in error by more than 10% and may well be good to ~5%. Values of J_1 and J_2 are readily found which satisfy conditions (i) to (iii) to better than 5% and are also within the limits set by (iv). The "best-fit" values for the exchange parameters are close to

$$J_1=10°\text{K}, \quad J_2=11°\text{K}, \quad (2.10)$$

giving a ratio $J_2/J_1=1.1$. This ratio is in excellent agreement with that measured by Coles, Orton, and Owen[34] for Mn^{++} pairs in MgO, which is $J_2/J_1=1.0\pm0.1$. The paramagnetic resonance pair spectrum, however, cannot be satisfactorily interpreted without the introduction of biquadratic exchange terms,[35] whose magnitudes are much larger than would seem possible (in view of the results of the present paper) for equivalent terms in MnO. We do not understand the reason for this discrepancy at the present time.

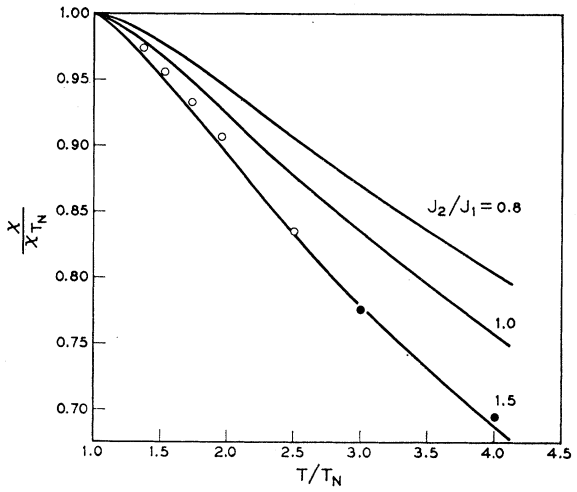

FIG. 5. The same as Fig. 3 but with the curves now plotted on a reduced scale making them independent of the absolute magnitude of exchange. The open circles are the experimental results of Lindsay (Ref. 32), the closed circles are those of Johnston and Heikes (Ref. 27).

3. THE ANTIFERROMAGNETIC STATE

Long range antiferromagnetic order sets in for MnO, with the fcc type-2 spin pattern, when the temperature is reduced to about 117°K. At and below this temperature, lattice distortions are observed, as described in Sec. 1. For MnO, the effects of isotropic volume contraction are very small compared with those of the rhombohedral deformation, and we shall neglect the former.[6]

Let the deformed cube have corner angles $\frac{1}{2}\pi\pm\Delta$. For small values of Δ, the distance d^+ between parallel pairs of nearest-neighbor spins and the distance d^-

[33] R. Kubo, Phys. Rev. **87**, 568 (1952).

[34] B. A. Coles, J. W. Orton, and J. Owen, Phys. Rev. Letters **4**, 116 (1960).

[35] E. A. Harris and J. Owen, Phys. Rev. Letters **11**, 9 (1963).

between antiparallel pairs of nearest-neighbor spins is

$$d^{\pm}=d(1\pm\tfrac{1}{2}\Delta), \tag{3.1}$$

where d is the nearest-neighbor distance in the cubic state.

In the same small Δ limit, we assume that the exchange interaction between d^- neighbors (J_1^+) and between the d^+ neighbors (J_1^-) may be written

$$J_1^{\pm}=J_1[1+\epsilon(d^{\pm}-d)/d]=J_1(1\pm\tfrac{1}{2}\epsilon\Delta), \tag{3.2}$$

where ϵ and Δ are positive if exchange decreases with increasing spin separation.

The free energy of the MnO system is dominantly made up of an exchange part F_{ex}, and an elastic part F_{el}. The former may be written in terms of the exchange Hamiltonian $\mathcal{H}$ as

$$F_{ex}=-kT\ln[\mathrm{tr}\exp(-\mathcal{H}/kT)], \tag{3.3}$$

where

$$\mathcal{H}=\sum_{nn}^{p}J_1^-\mathbf{S}_i\cdot\mathbf{S}_j+\sum_{nn}^{a}J_1^+\mathbf{S}_i\cdot\mathbf{S}_j+\sum_{nnn}J_2\mathbf{S}_i\cdot\mathbf{S}_j, \tag{3.4}$$

and where $\sum_{nn}{}^{p}$ and $\sum_{nn}{}^{a}$ refer to summations over nearest-neighbor parallel and antiparallel spin pairs, respectively. The elastic part of the free energy contains, in our approximation, a single shear term of the form

$$F_{el}=\tfrac{1}{2}C\Delta^2, \tag{3.5}$$

where $C(=3C_{44})$ has been measured, for MnO, by Oliver[36] and found to be 2.37×10^{12} dyne cm^{-2} to within about 5%.

The equilibrium situation is found by minimizing the total free energy with respect to Δ. Noting that

$$\partial F_{ex}/\partial\Delta=\langle\partial\mathcal{H}/\partial\Delta\rangle, \tag{3.6}$$

where the angular brackets denote a thermal average over the ensemble, the equilibrium condition becomes

$$\langle\partial\mathcal{H}/\partial\Delta\rangle+C\Delta=0. \tag{3.7}$$

Using Eqs. (3.2) and (3.4), this condition provides us with an expression for the equilibrium distortion Δ_{eq} in the form

$$\Delta_{eq}=Nz_1J_1\epsilon[\langle\mathbf{S}_i\cdot\mathbf{S}_j\rangle_{nn}{}^{p}-\langle\mathbf{S}_i\cdot\mathbf{S}_j\rangle_{nn}{}^{a}]/8C, \tag{3.8}$$

where $z_1(=12)$ is the number of nearest neighbors of any particular spin, where N is the number of spins in the system, and where $\langle\cdots\rangle_{nn}{}^{p}$ and $\langle\cdots\rangle_{nn}{}^{a}$ refer to thermal averages over parallel and antiparallel nearest neighbors, respectively.

The molecular-field estimate of Δ_{eq}, as obtained by Rodbell and Owen,[6] results (for $T<T_N$) from the approximation

$$\langle\mathbf{S}_i\cdot\mathbf{S}_j\rangle_{nn}{}^{p}=-\langle\mathbf{S}_i\cdot\mathbf{S}_j\rangle_{nn}{}^{a}=(\bar{S})^2, \tag{3.9}$$

and is

$$\Delta_{eq}=Nz_1J_1\epsilon(\bar{S})^2/4C. \tag{3.10}$$

Near the absolute zero of temperature, measurement of distortion finds that the parameter Δ_{eq} is close to 1.1×10^{-2} for MnO.[20] For temperatures above the Néel point it is zero.[15] If this last result is exact, it indicates, from (3.8), that $\langle\mathbf{S}_i\cdot\mathbf{S}_j\rangle_{nn}{}^{p}=\langle\mathbf{S}_i\cdot\mathbf{S}_j\rangle_{nn}{}^{a}$ throughout the paramagnetic region, in agreement with the Green's function calculations of Part I, but in disagreement with the interpretation of diffuse neutron-scattering measurements as given by Blech and Averbach.[37] We shall discuss this question in more detail in Sec. 6.

For temperatures between zero and T_N, the lattice strain varies closely as $(\bar{S})^2$ (Ref. 20), and would seem to indicate that the approximation (3.9) is a good one. This allows us to use with some confidence the relationship (3.10) in place of (3.8), and results in a considerable simplification of the associated statistical problem. Using the measured value of Δ_{eq} at zero temperature, together with the value of $\bar{S}(=2.43)$ which the spin-wave theory of Sec. 4 calculates for the average spin at 0°K, we find from Eq. (3.10), the result $J_1\epsilon\simeq230$°K. Inserting Δ_{eq} into the expression for the total (exchange plus strain) energy, we find that the system is described to a good approximation by (3.4), if

$$J_1^{\pm}=J_1\pm j(\bar{S})^2, \tag{3.11}$$

where $j=0.10k$, and where k is Boltzmann's constant. Thus, a nearest-neighbor distance change of $\sim\frac{1}{2}\%$ produces a change in exchange J_1 of $>5\%$.

The statistical problem is now completely defined except for the introduction of anisotropy terms which, however, are so small that they can be neglected outside the spin-wave region. The major "anomalous" feature of the magnetic properties of MnO in the antiferromagnetic state is the sublattice magnetization as a function of temperature. We shall calculate this magnetization using the Hamiltonian (3.4), where $J_1^{\pm}$ are given by (3.11), and neglecting anisotropy. Both the random-phase Green's function and the molecular-field approximations will be used so that their results may be compared.

In molecular-field theory, the sublattice magnetization may be written in terms of the Brillouin function (B_s) for spin S in the form

$$\bar{S}/S=B_s(g\mu_BSH_{eff}/kT), \tag{3.12}$$

where H_{eff} is the effective (or molecular) field acting on a typical spin $\mathbf{S}_i$, and is related to the interaction energy V of the spin with its time averaged surroundings by

$$H_{eff}=-V/g\mu_BS_i^z, \tag{3.13}$$

where z is the axis of spin alignment. For the case of MnO and Hamiltonian (3.4), we have

$$V=S_i^z\bar{S}(6J_1^--6J_1^+-6J_2), \tag{3.14}$$

[36] D. W. Oliver (private communication).

[37] I. A. Blech and B. L. Averbach, Physics 1, 31 (1964).

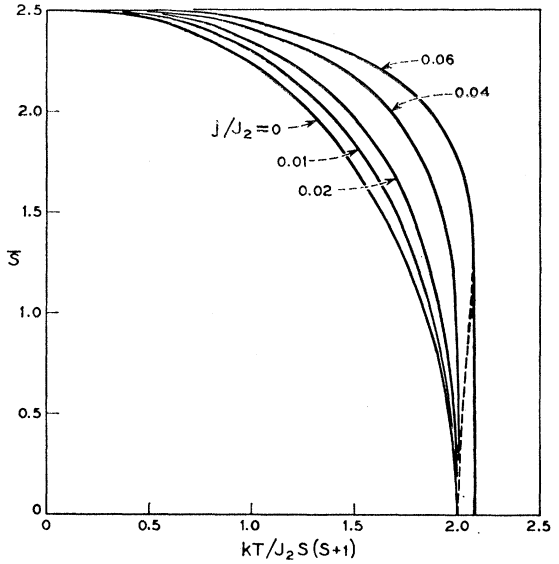

FIG. 6. Average spin per site $\bar{S}$ as a function of temperature, calculated in the molecular-field approximation [Eq. (3.16)] for spin $\frac{5}{2}$ and for various values of the distortion parameter j/J_2. The curves are independent of nearest-neighbor exchange J_1.

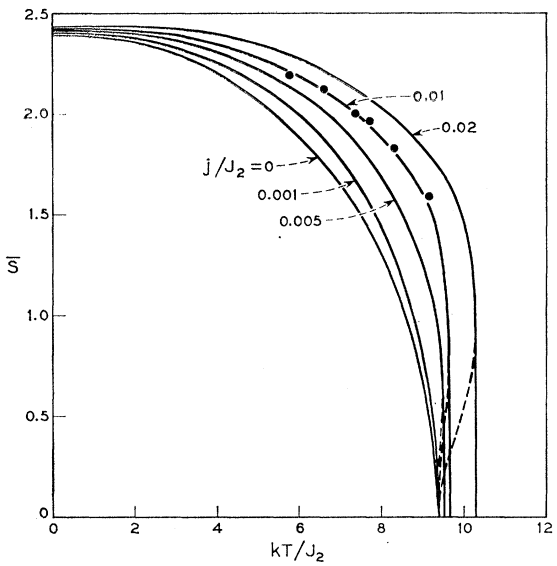

FIG. 7. Average spin per site $\bar{S}$ as a function of temperature, calculated in the random-phase Green's function approximation [Eqs. (3.17) and (3.18)] for spin $\frac{5}{2}$, for $J_2=J_1$, and for various values of distortion parameter. The closed circles are the experimental results of Shull, Strausser, and Wollan (Ref. 8).

from which it follows that

$$\bar{S}/S=B_s[6S\bar{S}(J_2+J_1^+-J_1^-)/kT]. \quad (3.15)$$

Using Eq. (3.11), we find a molecular-field implicit equation for $\bar{S}$ in the form

$$\bar{S}/S=B_s[6S\bar{S}(J_2+2j(\bar{S})^2)/kT]. \quad (3.16)$$

The solutions of this equation for $S=\frac{5}{2}$ are shown in Fig. 6, where average spin $\bar{S}$ is plotted against kT/J_2 for various values of the parameter j/J_2. These curves differ from those of Rodbell *et al.*,[1] who also attempted a molecular-field solution of the problem, because of an error in the interpretation of *their* Eq. (4). It would appear that their curves result from the assumption that the function $F(\sigma)$ of Eq. (4) is independent of j_1 and j_2 (their notation), which is not the case.

The shape of the sublattice spin vs temperature curve which is measured by neutron diffraction techniques[8] for MnO, is close to the $j/J_2=0.04$ curve of Fig. 6. [The equivalent result from Ref. 1 (putting $j_2=0$ and $j_1=j$) is $j/J_2\sim0.023$]. This is to be compared with the value $j/J_2=0.009$ which is the contribution to be expected from the rhombohedral distortion.

Now let us consider the results of Green's function theory. In the random-phase Green's function approximation, the sublattice magnetization as a function of temperature is given[23] by

$$\bar{S}/S=B_s(2S\coth^{-1}x), \quad (3.17)$$

where

$$x=\left\langle\frac{\mu}{[\mu^2-\lambda^2]^{1/2}}\coth\left[\frac{\bar{S}(\mu^2-\lambda^2)^{1/2}}{2kT}\right]\right\rangle_{\mathbf{K}}, \quad (3.18)$$

and where $\langle\cdots\rangle_{\mathbf{K}}$ is an average for the reciprocal lattice vector $\mathbf{K}$ running over values allowed by periodic boundary conditions in the first Brillouin zone of the reciprocal sublattice. The functions μ and λ are given in Part I for the case of MnO, but no allowance is made for lattice distortion. The modification required to include the distortion is very simple indeed. It is merely necessary to replace J_1 by J_1^- or J_1^+ in the expressions for μ and λ, depending upon whether the nearest-neighbor pairs are on the same or different sublattices respectively [Eqs. (2.4), (2.5), and (2.6) of Part I]. The resulting expressions for μ and λ are given by

$$\mu+\lambda=4J_1(c_1c_2+c_2c_3+c_3c_1)+4J_2(c_1^2+c_2^2+c_3^2)+4j(\bar{S})^2(3-s_1s_2-s_2s_3-s_3s_1), \quad (3.19)$$

$$\mu-\lambda=4J_1(s_1s_2+s_2s_3+s_3s_1)+4J_2(s_1^2+s_2^2+s_3^2)+4j(\bar{S})^2(3-c_1c_2-c_2c_3-c_3c_1), \quad (3.20)$$

where c_i and s_i $(i=1, 2, 3)$ are defined in Part I, and are the cosines and sines of three variables which in (3.18) may each be taken to run independently between $-\pi$ and π.

Solutions of (3.17), unlike those of (3.16), depend upon J_1. We have considered the case $J_1=J_2$ to be fairly representative of the situation for MnO and, using the computer to evaluate the averages $\langle\cdots\rangle_{\mathbf{K}}$, we have solved (3.17) for $\bar{S}$ as a function of kT/J_2 for the case $S=\frac{5}{2}$, and for a series of values j/J_2. The results are shown in Fig. 7 and are to be contrasted with the molecular-field estimates of Fig. 6. They suggest that the latter grossly underestimates the

effects of lattice distortion on the curve shape, particularly so for very small values of j. For example, the Green's function curve $j/J_2=0.001$ corresponds closely in shape to the molecular-field curve with distortion parameter ten times as large. Although the random-phase Green's function approximation may itself be of questionable validity,[25] especially for temperatures very close to T_N, the breakdown of molecular-field theory for the present case is confirmed (for $T<\frac{1}{2}T_N$) by the spin-wave calculation of Sec. 4.

From Fig. 7 we see that for all except the very small values of j/J_2, the transition at T_N is of first order (the sublattice magnetization coming to zero discontinuously). The critical value of j/J_2 for which the transition changes from second to first order has not been calculated, but it is certainly below 0.005. Thus, the transition in MnO should be of first order even if there is no real biquadratic exchange in the system. This would seem to be consistent with the experimental specific-heat data for MnO, which show an anomalously large peak at T_N and may include a small latent heat. The dashed parts of the curves in Figs. 6 and 7 are solutions which are energetically unstable.

At the present time, no published experimental information is available for MnO concerning the absolute value of sublattice spin as a function of temperature. Shull, Strausser, and Wollan,[8] however, have measured the temperature dependence of the intensity of neutron scattering from the [111] planes in MnO, and this intensity should be closely proportional to the square of the sublattice magnetization. The published measurements range from T_N down to nearly $\frac{1}{2}T_N$, but have not, unfortunately, been normalized at low temperatures. In Fig. 7 we show that they can be fitted very well to the $j/J_2=0.01$ curve, which is close to the value expected to arise from the MnO distortion. However, a good fit may also be obtained for somewhat larger values of j/J_2 (≈ 0.02) because the curves, as functions of T/T_N, are rather insensitive to distortion when $j/J_2>0.01$. In the absence of more detailed experimental information, it is not possible to discount these larger values.

With this difficulty in mind, it was decided to measure the temperature dependence of sublattice magnetization at very low temperatures. This has been done by studying the Mn^{55} zero-field nuclear magnetic resonance (NMR) in the antiferromagnetic state of MnO. The temperature dependence of the zero-field NMR has been observed at temperatures between 1.5 and 27°K (the experiment is described in detail in Sec. 5), and enables a measure of $\bar{S}_{T\to 0}-\bar{S}$ to be obtained in this low-temperature region. These results are particularly valuable because they are observed for a range of temperature where simple spin-wave theory should be an excellent approximation. Such a theory can be developed to include the effects of anisotropy which have so far been neglected, and will almost certainly give results of better accuracy than can be obtained by the use of Green's-function theory in the $\frac{1}{2}T_N \rightarrow T_N$ temperature region.

4. SPIN-WAVE THEORY AND SUBLATTICE MAGNETIZATION

In this section we shall develop a simple noninteracting spin-wave theory for MnO. We shall consider, in particular, the small deviation of sublattice magnetization from its value at absolute zero. At very low temperatures, this deviation depends significantly on anisotropy, and it is important that such terms are included even in salts which, like MnO, have anisotropy energies which amount to only a few percent of the isotropic exchange energy.

The origins of the major sources of anisotropy in MnO have been discussed by Keffer and O'Sullivan.[10] As discussed in Sec. 1, the largest contribution to anisotropy is probably that from dipole-dipole interactions, which constrains the spins to lie in [111] planes. Other smaller sources of anisotropy will add to this "out-of-plane" anisotropy, and will also give rise to an "in-plane" anisotropy which should pin down the spins to certain preferred orientations within the [111] planes. In this paper we shall not concern ourselves with the detailed forms of such anisotropy contributions, but we shall simply represent them by effective anisotropy fields. With this approximation we may write the spin-wave Hamiltonian for MnO [compare (3.4)] as

$$\mathcal{H}=\sum_{\text{nn}}^{p} J_1^{-}\mathbf{S}_i\cdot\mathbf{S}_j+\sum_{\text{nn}}^{a} J_1^{+}\mathbf{S}_i\cdot\mathbf{S}_j+\sum_{\text{nnn}} J_2\mathbf{S}_i\cdot\mathbf{S}_j +\sum_{\text{n}} D_1 S_{ix}^2+\sum_{\text{n}} D_2 S_{iy}^2, \quad (4.1)$$

where $\sum_{\text{n}}$ runs over all the spins in the lattice, where y and x are directions which are both normal to the direction z of spin alignment and are respectively parallel and perpendicular to a [111] plane, and where D_1 and D_2 are parameters which give a measure of "out-of-plane" and "in-plane" anisotropy, respectively. These parameters D_i are related to the "out-of-plane" and "in-plane" anisotropy energies K_1 and K_2 by the equations

$$D_i=3K_i/2NS^2, \quad (i=1, 2) \quad (4.2)$$

where N is the number of spins in the system.

Introducing the spin-wave creation and annihilation operators of Holstein and Primakoff[38] for the "up" sublattice (j) and the "down" sublattice (k) in the form

$$S_{jz}=S-a_j^{*}a_j, \qquad S_j^{+}=(2S)^{1/2}a_j, \qquad S_j^{-}=(2S)^{1/2}a_j^{*}; \quad (4.3)$$

$$S_{kz}=-S+b_k^{*}b_k, \quad S_k^{+}=(2S)^{1/2}b_k^{*}, \qquad S_k^{-}=(2S)^{1/2}b_k; \quad (4.4)$$

[38] T. Holstein and H. Primakoff, Phys. Rev. **58**, 1098 (1940).

where S is the spin quantum number, and where $S^{\pm}=S_x\pm iS_y$, the Hamiltonian (4.1) may be diagonalized by use of the transformations

$$\text{(i)}\quad \sqrt{2}a_j=Q_j+iP_j,\quad \sqrt{2}b_k=R_k+iS_k,\quad \sqrt{2}a_j^*=Q_j-iP_j,\quad \sqrt{2}b_k^*=R_k-iS_k; \tag{4.5}$$

$$\text{(ii)}\quad Q_j=(2/N)^{1/2}\sum_{\mathbf{K}} Q_{\mathbf{K}}e^{i\mathbf{K}\cdot\mathbf{j}},\quad P_j=(2/N)^{1/2}\sum_{\mathbf{K}} P_{\mathbf{K}}e^{-i\mathbf{K}\cdot\mathbf{j}},\quad R_k=(2/N)^{1/2}\sum_{\mathbf{K}} R_{\mathbf{K}}e^{-i\mathbf{K}\cdot\mathbf{k}},\quad S_k=(2/N)^{1/2}\sum_{\mathbf{K}} S_{\mathbf{K}}e^{i\mathbf{K}\cdot\mathbf{k}}; \tag{4.6}$$

where $\mathbf{K}$ is a reciprocal lattice vector which takes values determined by periodic boundary conditions and runs over $\frac{1}{2}N$ points in the first Brillouin zone of the reciprocal sublattice, and

$$\text{(iii)}\quad \begin{aligned} Q_{\mathbf{K}}&=\tfrac{1}{2}\sigma(q_{1,\mathbf{K}}+q_{2,\mathbf{K}}+iq_{1,-\mathbf{K}}+iq_{2,-\mathbf{K}}),\\ R_{\mathbf{K}}&=\tfrac{1}{2}\sigma(q_{1,-\mathbf{K}}-q_{2,-\mathbf{K}}+iq_{1,\mathbf{K}}-iq_{2,\mathbf{K}}),\\ P_{\mathbf{K}}&=\tfrac{1}{2}\sigma(p_{1,-\mathbf{K}}+p_{2,-\mathbf{K}}+ip_{1,\mathbf{K}}+ip_{2,\mathbf{K}}),\\ S_{\mathbf{K}}&=\tfrac{1}{2}\sigma(p_{1,\mathbf{K}}-p_{2,\mathbf{K}}+ip_{1,-\mathbf{K}}-ip_{2,-\mathbf{K}}); \end{aligned} \tag{4.7}$$

where $\sigma^2=-i$. In its normal coordinate form, the Hamiltonian now appears as

$$\begin{aligned}\mathcal{H}=&-\tfrac{1}{2}NS(S+1)[z_2J_2+\tfrac{1}{2}z_1(J_1^{+}-J_1^{-})]\\ &+\tfrac{1}{2}S\sum_{\mathbf{K}}\{(\beta_1+\gamma)q_{1,\mathbf{K}}^2+(\beta_2-\gamma)p_{1,\mathbf{K}}^2\\ &+(\beta_1-\gamma)q_{2,\mathbf{K}}^2+(\beta_2+\gamma)p_{2,\mathbf{K}}^2\},\end{aligned} \tag{4.8}$$

where the q and p coordinates satisfy the familiar position-momentum commutation relationships, where $z_1(=12)$ and $z_2(=6)$ are the number of nearest and next-nearest neighbors of any particular spin, and where

$$\beta_1=\sum_{\mathrm{nn}}^{p} J_1^{-}e^{i\mathbf{K}\cdot(\mathbf{r}-\mathbf{r}_0)}+z_2J_2+\tfrac{1}{2}z_1(J_1^{+}-J_1^{-})+2D_1, \tag{4.9}$$

$$\beta_2=\sum_{\mathrm{nn}}^{p} J_1^{-}e^{i\mathbf{K}\cdot(\mathbf{r}-\mathbf{r}_0)}+z_2J_2+\tfrac{1}{2}z_1(J_1^{+}-J_1^{-})+2D_2, \tag{4.10}$$

$$\gamma=\sum_{\mathrm{nn}}^{a} J_1^{+}e^{i\mathbf{K}\cdot(\mathbf{r}-\mathbf{r}_0)}+\sum_{\mathrm{nnn}} J_2e^{i\mathbf{K}\cdot(\mathbf{r}-\mathbf{r}_0)}. \tag{4.11}$$

In these equations, $\sum_{\mathrm{nn}}{}^{p}$ ($\sum_{\mathrm{nn}}{}^{a}$) runs over all parallel (antiparallel) nearest neighbors $\mathbf{r}$ of $\mathbf{r}_0$, and $\sum_{\mathrm{nnn}}$ runs over all next-nearest neighbors $\mathbf{r}$ of $\mathbf{r}_0$.

The eigenvalues of (4.8) may be written

$$\begin{aligned}E_{n_1n_2}=&-\tfrac{1}{2}NS(S+1)[z_2J_2+\tfrac{1}{2}z_1(J_1^{+}-J_1^{-})]\\ &+\sum_{\mathbf{K}}\{(n_{1\mathbf{K}}+\tfrac{1}{2})\hbar\omega_{1\mathbf{K}}+(n_{2\mathbf{K}}+\tfrac{1}{2})\hbar\omega_{2\mathbf{K}}\},\end{aligned} \tag{4.12}$$

where $n_{1\mathbf{K}}$ and $n_{2\mathbf{K}}$ are positive integers denoting the number of spin waves with wave vector $\mathbf{K}$ and frequencies $\omega_{1\mathbf{K}}$ and $\omega_{2\mathbf{K}}$ respectively, and where

$$\hbar\omega_{1\mathbf{K}}=S[(\beta_1+\gamma)(\beta_2-\gamma)]^{1/2}, \tag{4.13}$$

$$\hbar\omega_{2\mathbf{K}}=S[(\beta_1-\gamma)(\beta_2+\gamma)]^{1/2} \tag{4.14}$$

are the spin-wave energies.

The z component of spin $\mathbf{S}_j$ is given by Eq. (4.3). Using the transformations (4.5) to (4.7) we find

$$\bar{S}_{jz}=S+\tfrac{1}{2}-(1/2N)\times\sum_{\mathbf{K}}\langle(q_{1,\mathbf{K}}^2+q_{2,\mathbf{K}}^2+p_{1,\mathbf{K}}^2+p_{2,\mathbf{K}}^2)\rangle, \tag{4.15}$$

where the angular bracket represents a thermal average over the ensemble, and where we have put terms $\langle q_{1,\mathbf{K}}q_{2,\mathbf{K}}\rangle$ and $\langle p_{1,\mathbf{K}}p_{2,\mathbf{K}}\rangle$ equal to zero because of the orthogonality of the oscillators (q_1,p_1) and (q_2,p_2). Using the fact that the average values of kinetic and potential energy for a harmonic oscillator are equal, we find from (4.8) and (4.12), that

$$\langle q_{1,\mathbf{K}}^2\rangle=\langle n_{1\mathbf{K}}+\tfrac{1}{2}\rangle[(\beta_2-\gamma)/(\beta_1+\gamma)]^{1/2}, \tag{4.16}$$

$$\langle p_{1,\mathbf{K}}^2\rangle=\langle n_{1\mathbf{K}}+\tfrac{1}{2}\rangle[(\beta_1+\gamma)/(\beta_2-\gamma)]^{1/2}, \tag{4.17}$$

together with similar equations for $\langle q_{2,\mathbf{K}}^2\rangle$ and $\langle p_{2,\mathbf{K}}^2\rangle$ which result from the above equations by changing the sign of γ. From the knowledge of the boson distribution function, the ensemble average $\langle n_{i\mathbf{K}}+\frac{1}{2}\rangle$ is readily calculated to be

$$\langle n_{i\mathbf{K}}+\tfrac{1}{2}\rangle=\tfrac{1}{2}\coth(\hbar\omega_{i\mathbf{K}}/2kT)\quad (i=1,2). \tag{4.18}$$

The resulting expression for the average sublattice spin per site $\bar{S}$ follows from Eqs. (4.13) to (4.18), and is

$$\bar{S}=S+\tfrac{1}{2}-\tfrac{1}{4}\left\langle\frac{\beta_1+\beta_2}{[(\beta_1+\gamma)(\beta_2-\gamma)]^{1/2}}\times\coth\left[\frac{S[(\beta_1+\gamma)(\beta_2-\gamma)]^{1/2}}{2kT}\right]\right\rangle_{\mathbf{K}}, \tag{4.19}$$

where, from (4.9) to (4.11),

$$\beta_1+\gamma=\mu+\lambda+2D_1, \tag{4.20}$$

$$\beta_2-\gamma=\mu-\lambda+2D_2, \tag{4.21}$$

where μ and λ are defined in (3.19) and (3.20), and where we have used, in obtaining (4.19), the fact that the average over $\mathbf{K}$ is unchanged when the subscripts 1 and 2 are interchanged. For a numerical calculation we require to know the values of J_1, J_2, j, D_1, and D_2. For the first three parameters we use the estimates obtained earlier. Thus, for J_1 and J_2 we take values 10 and 11°K, respectively, which are probably good to $\sim\pm5\%$. For j we use the value 0.10°K as calculated from the observed lattice distortion. It, too, is probably accurate to better than 10%. A measure of D_1 can be obtained from the antiferromagnetic resonance fre-

quency (27.5 cm^{-1}) which has been observed by Sievers and Tinkham[19] and Richards.[39]

There should be two different antiferromagnetic resonance frequencies for MnO, associated with the two different spin-wave branches of Eqs. (4.13) and (4.14). As yet, only one of the resonances has been observed, and it would appear to be associated with the "out-of-plane" anisotropy which is mainly of dipolar origin. This resonance frequency may be expressed in terms of the anisotropy energy K_1 and the perpendicular susceptibility $\chi_\perp(T=0)$ in the form

$$\hbar\omega_{afmr}=g\mu_B(3K_1/\chi_\perp)^{1/2}, \tag{4.22}$$

from which [using[1] $\chi_\perp(T=0)=(74\pm5)10^{-6}$ emu/g], we find a value $K_1=(1.16\pm0.08)10^7$ ergs/cm^3, which is to be compared with the classical dipole-dipole estimate[14] of 1.64×10^7 ergs/cm^3. It is better, however, to compare with a classical estimate reduced to allow for the 3% spin-wave reduction of $\bar{S}$ from $\frac{5}{2}$ which we shall find for MnO. The numerical coefficient is then reduced to 1.54. The effects of lattice distortion on this dipole-dipole calculation are very small,[10] so that the difference between the above estimates may well give an indication of the magnitude and sign of the nondipolar contributions to the "out-of-plane" anisotropy. Using the value of K_1 calculated from (4.22), we find $D_1=(0.44\pm0.03)$°K. If we identify the antiferromagnetic resonance frequency with the zero wave-vector mode ω_{2K} of Eq. (4.14), then we calculate a value $D_1=0.48$°K. For use in the computation to be carried out for $\bar{S}$, we take the parameter D_1 equal to 0.46°K.

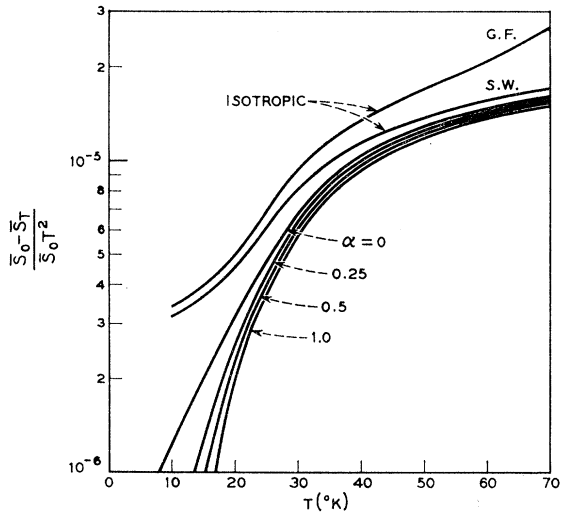

FIG. 8. Spin deviation from its value at absolute zero plotted as a function of temperature, as calculated in the simple spin-wave approximation from Eq. (4.19)with $J_1=10$°K, $J_2=11$°K, $j=0.10$°K, $D_1=0.46$°K, and $D_2=\alpha D_1$. Also shown are the isotropic curves $D_1=D_2=0$, calculated by spin-wave theory (S. W.) and by Green's function theory (G. F.).

Little is known at present about D_2 except that it is likely to be considerably smaller than D_1. Keffer and O'Sullivan[10] have considered the field dependence of powder susceptibility and have interpreted the experimental evidence in terms of a model in which the "in-plane" anisotropy is much smaller than the "out-of-plane" anisotropy. They favor a value for D_2 which is about two orders of magnitude smaller than D_1.

In Fig. 8 we show the results obtained by computing $\bar{S}$ self-consistently from (4.19). Curves of spin deviation from the zero-temperature state ($\bar{S}_0$) are plotted as a function of temperature for the above-mentioned values of J_1, J_2, j, and D_1, and for various values of $D_2\leq D_1$. Also shown is the isotropic result $D_1=D_2=0$, which has been calculated both by spin-wave and random-phase Green's function methods. The latter approach renormalizes the spin-wave energies to the sublattice magnetization and, in the very low-temperature region where the spin-wave interactions are small, results in spin deviations which are too large. At higher temperatures where the interactions between spin waves are important, the Green's function method takes over as the better approximation because all spin-wave interactions have been neglected in the theory of this section. The temperature region where the two isotropic curves of Fig. 8 begin to differ significantly in shape should, therefore, be an estimate of the temperature where simple spin-wave theory breaks down and where spin-wave interactions begin to be important. For MnO this occurs when $T\sim50$ to 60°K, which is $T\sim\frac{1}{2}T_N$. This is a somewhat larger fraction of the Néel temperature than was found for the breakdown of simple spin-wave theory in MnF_2,[40] and is due to the distortion effect which reduces the number of spin waves in the MnO system below what it would be in a more rigid system (MnF_2) at the same fraction of the Néel temperature.

The value of sublattice spin $\bar{S}_0$ at $T=0$°K is very insensitive to the unknown parameter D_2, and ranges from a value 2.425 when D_2 is zero, to 2.427 when $D_2=D_1$. This represents a zero-point spin deviation (from the $S=\frac{5}{2}$ Néel state) of 2.9 to 3.0%.

5. Mn^{55} ZERO-FIELD NMR IN ANTIFERROMAGNETIC MnO

In this section, we present the results and interpretation of the observation of the Mn^{55} zero-field NMR in the antiferromagnetic state of MnO. We find that a determination of the average sublattice spin in the antiferromagnetic ground state at 0°K is not possible because of an apparent increase of the hyperfine coupling constant A^{55} in MnO over the value determined by electron paramagnetic resonance (EPR) of Mn^{++}:MgO. From the measured temperature dependence of the Mn^{55} zero-field NMR frequency, we are able to com-

[39] P. L. Richards, J. Appl. Phys. 34, 1237 (1963).

[40] V. Jaccarino, in *Magnetism*, edited by G. Rado and H. Suhl (Academic Press, Inc., New York, 1963), Vol. 2.

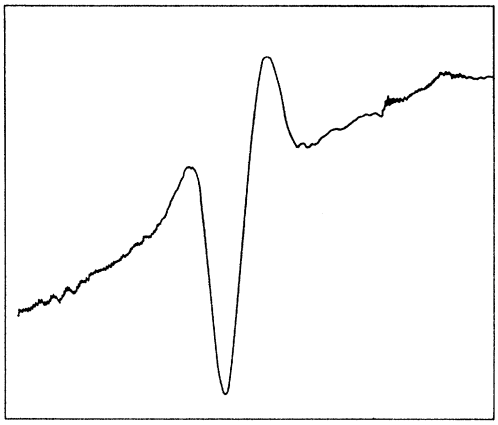

FIG. 9. Tracing of the second derivative Mn^{55} zero-field NMR in antiferromagnetic MnO at $T=1.5°K$.

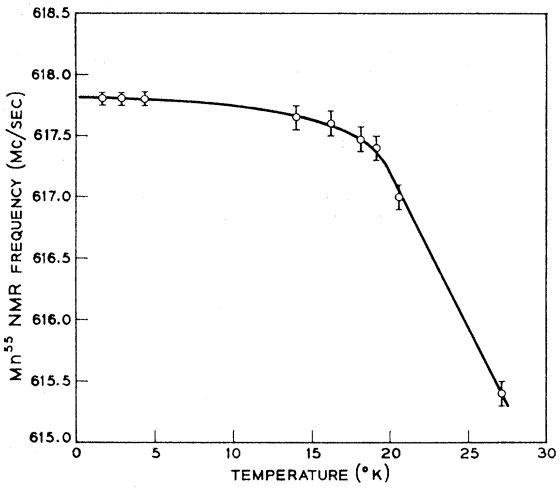

FIG. 10. Temperature dependence of the zero-field Mn^{55} NMR frequency in antiferromagnetic MnO.

pare the calculated and experimentally measured temperature dependence of sublattice magnetization. In the last part of this section, we present the results of an indirect nuclear spin-spin interaction calculation, applicable to MnO, and experimentally measured from the Mn^{55} zero-field NMR linewidth data.

Experimental

The zero-field Mn^{55} NMR was observed in a powdered sample of MnO in the frequency range of 615 to 618 Mc/sec between 1.5 and 27.1°K. The NMR spectrometers used to observe the resonance were a cw and a super-regenerative uhf oscillator described in detail by Jefferts and Jones.[41] Using the cw spectrometer, the Mn^{55} NMR was observable up to 4.2°K, while with the super-regenerative oscillator the Mn^{55} NMR was observable up to 27.1°K (liquid neon). A search for the Mn^{55} NMR was conducted at 64°K, but with negative results. The experimental procedure and technique for observing this type of NMR have been treated in detail elsewhere.[41,42]

Mn^{55} NMR in Antiferromagnetic MnO

A typical 1.5°K zero-field Mn^{55} NMR, obtained with the cw spectrometer, is shown in Fig. 9. Because of excessive modulation pickup, second-harmonic detection techniques were used. The peak-to-peak absorption derivative linewidth is the distance between zero crossings of the Mn^{55} NMR shown in Fig. 9, and was measured to be $\delta H \approx 540$ Oe ($\delta\nu \approx 560$ kc/sec). The Mn^{55} NMR frequency for this temperature was measured to be $\nu^{55}(1.5°K)=617.8\pm0.1$ Mc/sec. We attribute the distortion of the Mn^{55} NMR line shape to nonlinear effects of the cw spectrometer. The result of subtracting a nonlinear base line from the NMR spectrum (shown in Fig. 9), suggests that the line shape is probably Gaussian. We note that the strain which is present in MnO for $T<T_N$, has not introduced any appreciable contribution to the Mn^{55} NMR line shape by quadrupolar interactions. The measured temperature dependence of the Mn^{55} NMR frequency is shown in Fig. 10. A smooth curve has been drawn through the experimental points and extrapolating the data to 0°K yields a value $\nu^{55}(0)=617.8\pm0.1$ Mc/sec.

The zero-field time-independent Hamiltonian for a given Mn^{55} nucleus in antiferromagnetic MnO can be written as[43]

$$\mathcal{H}=A_z^{55}\langle S_z\rangle I_z+\gamma^{55}\hbar I_z\sum_i D_z{}^i\langle S_z{}^i\rangle, \qquad (5.1)$$

where the z axis has been taken to be the direction of the sublattice magnetization, $\langle S_z\rangle=\bar{S}$ is the time averaged electron spin polarization per Mn^{++} ion, A^{55} the magnetic hyperfine coupling constant, I the nuclear spin ($I=\frac{5}{2}$), and γ^{55} the Mn^{55} nuclear gyromagnetic ratio. The second term in Eq. (5.1) is the magnetic interaction between the Mn^{55} nuclear moment and the dipolar field due to the neighboring electronic spins, $H_{\rm dip}=\sum_i D_z{}^i\langle S_z{}^i\rangle$, where i is summed over all lattice points. This dipolar field is not a result of the small rhombic distortion in MnO which removes the cubic symmetry of the crystal for $T<T_N$, but is a result of the type-2 antiferromagnetic order. We have calculated the D tensor with the result $H_{\rm dip}=+7.67$ kOe for $\bar{S}=\frac{5}{2}$, where the plus sign means that it is in the same direction as the Mn^{++} electron magnetic moment. As previously mentioned, there is no indication of an appreciable quadrupolar interaction and thus we have not included this interaction in Eq. (5.1).

The Mn^{55} zero-field NMR frequency $\nu^{55}(T)$ is easily

[41] K. B. Jefferts and E. D. Jones, Rev. Sci. Instr. (to be published).

[42] E. D. Jones and K. B. Jefferts, Phys. Rev. **135**, A1277 (1964).

[43] T. Moriya, Progr. Theoret. Phys. (Kyoto) **16**, 641 (1956).

derived from the Hamiltonian (5.1) with the result

$$\nu^{55}(T)=\{(\tfrac{5}{2})|A^{55}/h|-(\gamma^{55}/2\pi)H_{\rm dip}\}\bar{S}/S, \quad (5.2)$$

where we have assumed that A^{55} is negative and large compared to $\gamma^{55}\hbar H_{\rm dip}$. We further assume that the temperature dependence of the hyperfine coupling constant is negligible in the temperature range for which we observe the Mn^{55} zero-field NMR (see Table I). Thus, the temperature dependence of $\nu^{55}(T)$ is contained in the time averaged electron spin $\bar{S}$.

Normally at this time, we should be able to calculate the effect that the zero-point spin fluctuations have upon the ground state spin alignment at 0°K. This was accomplished[42] for antiferromagnetic MnF_2 by combining the measured $\nu^{55}(0)$ with the value for A^{55} (determined by EPR of Mn^{++}:ZnF_2) and the calculated dipolar field, and then solving for $\bar{S}/S$. However, for MnO, this procedure leads to difficulties which are as follows. Let us, for the moment, assume that there is no zero-point spin reduction, i.e., $\bar{S}=S$, and calculate the value for A^{55} from Eq. (5.2) using $\nu^{55}(0)=617.8\pm0.1$ Mc/sec and $H_{\rm dip}=+7.67$ kOe. The result of this calculation is $A^{55}=-(83.51\pm0.01)10^{-4}$ cm^{-1}. Listed in Table I are various values of A^{55} determined by the EPR of the Mn^{++} ion in the nonmagnetic isomorphs of MnO. We see that, in all cases, the hyperfine coupling constant A^{55} as determined by the EPR method is about 2–3% smaller than the value which we calculated above for the case of no zero-point spin reduction. Including a zero-point spin reduction of $1-\bar{S}/S\approx3\%$, as calculated in section 4 for MnO, only increases this discrepancy for A^{55} determined by the two different types of measurements. Since, at the present time, we have no reason to include any new interactions into Eq. (5.1), we cannot make any conclusions regarding the magnitude of the zero-point spin reduction in MnO until the question concerning the value of A^{55} is resolved.

TABLE I. Comparison of Mn^{2+} hyperfine coupling constants for 6-fold cubic oxygen coordination.

Lattice	Lattice constant (Å)	Temperature (°K)	A (cm$^{-1}\times10^4$)	Reference
MgO	4.203	290	−81.2±0.05	a
		4.2	−81.55	a
CaO	4.797	290	−80.7±0.1	b,c
		77	−81.6	b
		20	−81.7	b
		4.2	−81.7	b
SrO	5.10	290	−78.1±0.2	c
		77	−80.2	c
		4.2	−80.7	c
MnO	4.435	150–300	−81.5±1.6	d

[a] W. M. Walsh, Jr. (private communication).
[b] W. Low and R. S. Rubins, *Proceedings of the First International Conference on Paramagnetic Resonance*, edited by W. Low (Academic Press Inc., New York, 1963).
[c] A. J. Shuskus, Jr., Chem. Phys. **41**, 1885 (1964).
[d] E. D. Jones, J. Appl. Phys. (to be published).

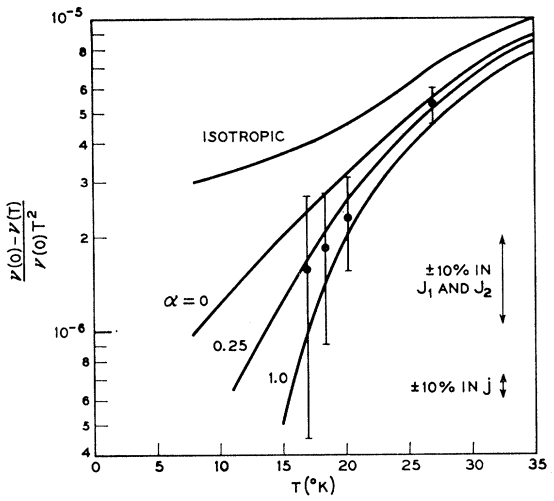

FIG. 11. The theoretical spin deviation results of Fig. 8 are compared with the experimental temperature dependence of Mn^{55} NMR frequency (see text). The error in the experimental measurements is given by the brackets on the data. Also indicated is the sensitivity of the theoretical curves to small variations in J_1 and J_2 (together) and in j.

From Eq. (5.2), it is evident that $\nu^{55}(T)\propto\bar{S}(T)$. It follows that $[\nu(0)-\nu(T)]/\nu(0)=[\bar{S}(0)-\bar{S}(T)]/\bar{S}(0)$. The experimental data are shown in Fig. 11 where $[\nu(0)-\nu(T)]/\nu(0)T^2$ is plotted as a function of temperature. The error in the experimental measurements is given by the brackets on the data. Also shown in Fig. 11 are the theoretical spin-wave results as obtained in Sec. 4. The sensitivity of these curves to small variations in j and in bilinear exchange (about the chosen values) is also indicated (as a first approximation, the curves retain their shape under these variations). The sensitivity of spin deviation to distortion is very large indeed for small $j(\ll0.1°\text{K})$ but decreases with increasing j. Thus, at 10°K, the spin deviation in an undistorted MnO lattice would be ~10 times larger than it is in the $j=0.1°$K case of Fig. 11.

We find, in general, a good agreement between theory and experiment, but the combined effect of experimental error and uncertainty in the values to be taken for J_1 and J_2 are such that it is not possible to deduce anything about the "in-plane" anisotropy parameter D_2 from this data. The significant result is that the temperature variation of sublattice magnetization in the spin-wave region may be understood (as it was for temperatures closer to T_N) in the complete absence of real biquadratic exchange.

It is also true, however, that the spin-wave results do not completely exclude the possibility that small biquadratic terms could be present in the system, in addition to the distortion terms. We find that the low-temperature data may be fitted theoretically for values of j somewhat larger than 0.10°K. These larger values of j modify the calculated Néel temperature (see Fig. 7) and result in a slightly smaller value of J_2 being ob-

tained from the calculations of Sec. 2. The combined effects of a slightly decreased J_2 and an enhanced value of j tend to cancel out in Fig. 11. Since a real biquadratic exchange term would behave very much like an added distortion term in the ordered state, we conclude that the presence of such a term would not necessarily destroy the agreement between theory and experiment which has been obtained in this paper. Because of this situation, it is difficult to make any statement concerning an upper limit to the size of a possible biquadratic term. The fact remains, however, that we possess to date no experimental evidence on MnO which *requires* a biquadratic exchange for its theoretical interpretation.

Mn^{55} NMR Linewidth

The contribution to NMR linewidths in antiferromagnetic structures by the indirect nuclear spin-spin interaction has been discussed by Suhl[44] and Nakamura.[45] We now calculate this contribution to the Mn^{55} NMR linewidth in antiferromagnetic MnO, following Ref. 45.

The Hamiltonian for the electron-nuclear spin system is

$$\mathcal{H}=\mathcal{H}_0+\mathcal{H}', \tag{5.3}$$

where $\mathcal{H}_0$ is given by Eq. (4.1), and where $\mathcal{H}'$ is the interaction Hamiltonian between the nuclear and electron spin systems, and is written as

$$\mathcal{H}'=A\sum_n \mathbf{I}_n\cdot\mathbf{S}_n, \tag{5.4}$$

where A is the hyperfine interaction ($A^{55}=-83.5\times10^{-4}$ cm^{-1}). Considering only the transverse components, we write Eq. (5.4) in terms of the normal coordinates defined in Eqs. (4.5), (4.6), and (4.7), and obtain

$$\mathcal{H}'=(A^2S/8N)^{1/2}\sigma \times\sum_{\mathbf{K}}\{I_{\mathbf{K}}^+[(q_1-ip_1+q_2-ip_2)+i(q_1'-ip_1'+q_2'-ip_2')] +J_{\mathbf{K}}^+[(q_1+ip_1-q_2-ip_2)+i(q_1'+ip_1'-q_2'-ip_2')]\} +\text{complex conjugate}, \tag{5.5}$$

where

$$I_{\mathbf{K}}^+=\sum_j I_j^+e^{i\mathbf{K}\cdot\mathbf{j}}, \quad J_{\mathbf{K}}^+=\sum_k I_k^+e^{i\mathbf{K}\cdot\mathbf{k}}, \tag{5.6}$$

are the Fourier transformed operators of I_x+iI_y, and where

$$q_{1,\mathbf{K}}\equiv q_1, \quad q_{1,-\mathbf{K}}\equiv q_1', \quad \text{etc.} \tag{5.7}$$

A second-order perturbation calculation of Eq. (5.5) gives

$$E^{(2)}=-(A^2S^2/8NJ_1) \times\sum_{\mathbf{K}}\{(I_{\mathbf{K}}^+I_{\mathbf{K}}^-+I_{\mathbf{K}}^-I_{\mathbf{K}}^++J_{\mathbf{K}}^+J_{\mathbf{K}}^-+J_{\mathbf{K}}^-J_{\mathbf{K}}^+)X_{\mathbf{K}} -4(I_{\mathbf{K}}^+J_{\mathbf{K}}^-+I_{\mathbf{K}}^-J_{\mathbf{K}}^+)Y_{\mathbf{K}}\}, \tag{5.8}$$

with

$$X_{\mathbf{K}}=J_1(\beta_1+\beta_2)[1/(\hbar\omega_{1\mathbf{K}})^2+1/(\hbar\omega_{2\mathbf{K}})^2], \tag{5.9}$$

$$Y_{\mathbf{K}}=(J_1/2)\{(2\gamma+\beta_1-\beta_2)(\hbar\omega_{1\mathbf{K}})^{-2} +(2\gamma-\beta_1+\beta_2)(\hbar\omega_{2\mathbf{K}})^{-2}\}, \tag{5.10}$$

where γ, β_1, β_2, $\omega_{1\mathbf{K}}$, and $\omega_{2\mathbf{K}}$, are defined by Eqs. (4.9) to (4.14). Terms linear in I_z which lead to a shift of the Mn^{55} NMR frequency are not included in (5.8) because these terms are small compared with the corresponding terms arising from the longitudinal part of Eq. (5.4).

The effective nuclear spin Hamiltonian can thus be written as

$$\mathcal{H}_{\text{eff}}=\tfrac{1}{2}D[\sum_j (I_j^z)^2+\sum_k (I_k^z)^2] -\tfrac{1}{2}\sum_{j>j'} B_{jj'}(I_j^+I_{j'}^-+I_j^-I_{j'}^+) -\tfrac{1}{2}\sum_{k>k'} B_{kk'}(I_k^+I_{k'}^-+I_k^-I_{k'}^+) -\sum_{j,k} C_{jk}(I_j^+I_k^-+I_j^-I_k^+), \tag{5.11}$$

where

$$D=(A^2S^2/2J_1N)\sum_{\mathbf{K}} X_{\mathbf{K}}, \tag{5.12}$$

$$B_{jj'}=(A^2S^2/2J_1N)\sum_{\mathbf{K}} X_{\mathbf{K}}\cos[\mathbf{K}\cdot(\mathbf{j}-\mathbf{j}')], \tag{5.13}$$

$$C_{jk}=-(A^2S^2/2J_1N)\sum_{\mathbf{K}} Y_{\mathbf{K}}\cos[\mathbf{K}\cdot(\mathbf{j}-\mathbf{k})]. \tag{5.14}$$

These equations reduce to Nakamura's[45] for the case of a single exchange and uniaxial anisotropy.

We are now able to calculate an expression for the peak-to-peak Mn^{55} zero-field NMR linewidth from Eq. (5.11), with the result (see Ref. 45 for details)

$$\delta H=(A^2S^2/2hJ_1\gamma^{55})[(1/3)I(I+1)f +(1/20)(2I-1)(2I+3)f_0^2]^{1/2}, \tag{5.15}$$

where

$$f=\langle X_{\mathbf{K}}^2\rangle_{\mathbf{K}}, \quad f_0=\langle X_{\mathbf{K}}\rangle_{\mathbf{K}}. \tag{5.16}$$

For a numerical evaluation of f and f_0, we require the knowledge of J_1, J_2, j, D_1, and D_2. We use the estimates previously obtained for the first four quantities, i.e., 10, 11, 0.10, and 0.46°K, respectively. The functions f and f_0 are numerically calculated as a function of the inplane anisotropy D_2. The dependence of f_0 and f upon the ratio D_2/D_1 is shown graphically in Figs. 12 and 13.

[44] H. Suhl, Phys. Rev. **109**, 606 (1958); J. Phys. Radium **20**, 333 (1959).
[45] T. Nakamura, Progr. Theoret. Phys. (Kyoto) **20**, 542 (1958).

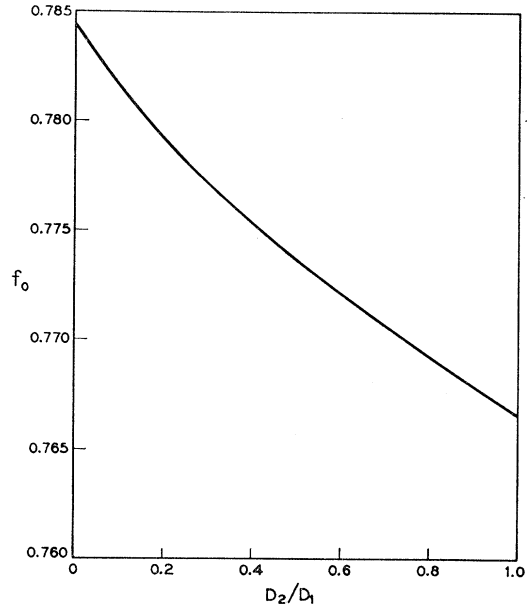

FIG. 12. The function f_0 of Eq. (5.16) as a function of the ratio of "in-plane" anisotropy D_2 to "out-of-plane" anisotropy D_1.

The peak-to-peak absorption derivative linewidth δH defined by Eq. (5.15) is shown in Fig. 14 as a function of D_2/D_1. Using the estimate of Keffer and O'Sullivan[10] that $D_2/D_1 \approx 10^{-2}$, Fig. 14 indicates a linewidth $\delta H \approx 380$ Oe. In order for the indirect nuclear spin-spin interaction to account for the observed linewidth of $H \approx 540$ Oe, we must use a value $D_2/D_1 \approx 10^{-3}$. However, we are not allowed to let D_2/D_1 become arbitrarily small, since for very small values of in-plane anisotropy, the Mn^{55} NMR frequency will be a function of the applied r.f. power.[46] Since we did not observe any frequency pulling effects, it seems probable that $D_2/D_1 > 10^{-3}$ and the preceding calculation may, therefore, not be able to account for the full observed linewidth (for $D_2/D_1 \approx 10^{-2}$ it accounts for approximately 70% of the observed NMR linewidth).

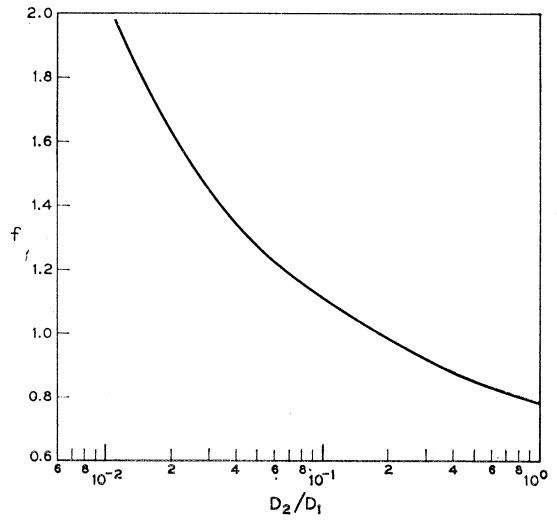

FIG. 13. The function f of Eq. (5.16) plotted as a function of D_2/D_1.

6. SHORT-RANGE ORDER IN THE PARAMAGNETIC STATE

In Part I of this paper, we used the random-phase Green's function approximation to calculate the near-neighbor spin correlations in the paramagnetic state of a fcc type-2 antiferromagnet. These calculations show that the nearest-neighbor correlations are all equal (and negative), and that they are in general considerably smaller than the next-nearest-neighbor correlations.

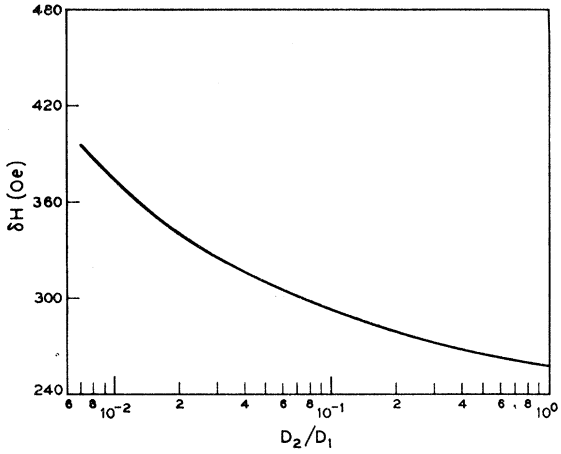

FIG. 14. The peak-to-peak absorption derivative linewidth [Eq. (5.15)] as a function of D_2/D_1.

Such a calculation is applicable to MnO only if we can show that the distortion mechanism (which is not considered in Part I) is inoperative in the paramagnetic state. The relationship between the equilibrium value of distortion Δ_{eq} and the nearest-neighbor spin correlations is given by (3.8). Thus, any observed rhombohedral distortion in the paramagnetic state would imply that the nearest-neighbor correlations were not all equal. No such distortion has yet been observed, but let us for the moment assume that it may be present, but too small to be easily observable.

From Eq. (4.9) of Part I, the nearest neighbor spin correlations can be written in terms of the exchange parameters $J_1^{\pm}$ and J_2. Expressing χ_0^{-1} in the form $12(J_1^{+}+J_2)+F(T-T_N)$, where $F(T-T_N)$ is a positive function increasing in magnitude with increasing temperature, we find that the two nearest-neighbor

[46] P. G. de Gennes, P. A. Pincus, F. Hartmann-Boutron, and J. M. Winter, Phys. Rev. 129, 1105 (1963).

correlations $\langle\cdots\rangle_{nn}{}^{p}$ and $\langle\cdots\rangle_{nn}{}^{a}$ can be written in the form

$$\langle \mathbf{S}_i\cdot\mathbf{S}_j\rangle_{nn}{}^{p}=3kT\langle(c_1c_2+s_1s_2)/[F(T-T_N)+\mu+\lambda]\rangle_K, \quad (6.1)$$

$$\langle \mathbf{S}_i\cdot\mathbf{S}_j\rangle_{nn}{}^{a}=3kT\langle(c_1c_2-s_1s_2)/[F(T-T_N)+\mu+\lambda]\rangle_K, \quad (6.2)$$

where $\mu+\lambda$ is given by Eq. (3.19) but with $4j(\bar{S})^2$ replaced by $2(J_1{}^{+}-J_1{}^{-})$. The superscripts p and a refer respectively to nearest-neighbor spin pairs associated with $J_1{}^{-}$ and $J_1{}^{+}$ exchange interactions.

From Eq. (3.8), using the measured value of the elastic constant C and the previously estimated value of $J_1\epsilon$, we find (for MnO)

$$\Delta_{eq}=9.2\times10^{-4}[\langle \mathbf{S}_i\cdot\mathbf{S}_j\rangle_{nn}{}^{p}-\langle \mathbf{S}_i\cdot\mathbf{S}_j\rangle_{nn}{}^{a}]. \quad (6.3)$$

Also, from (3.2), it follows that

$$J_1{}^{\pm}=J_1\pm0.10k[\langle \mathbf{S}_i\cdot\mathbf{S}_j\rangle_{nn}{}^{p}-\langle \mathbf{S}_i\cdot\mathbf{S}_j\rangle_{nn}{}^{a}] =J_1\pm115k\Delta_{eq}, \quad (6.4)$$

where k is Boltzmann's constant. Inserting (6.1) and (6.2) into (6.4), we derive a consistency condition for Δ_{eq}. It is

$$\langle s_1s_2/[F(T-T_N)+\mu+\lambda]\rangle_K=192\Delta_{eq}/kT, \quad (6.5)$$

where

$$\mu+\lambda=4J_1(c_1c_2+c_2c_3+c_3c_1)+4J_2(c_1{}^{2}+c_2{}^{2}+c_3{}^{2}) +230\Delta_{eq}(3-s_1s_2-s_2s_3-s_3s_1). \quad (6.6)$$

Physically meaningful solutions must, from (6.3), have $\Delta_{eq}\lesssim0.01$. Putting $J_1=10°K$, $J_2=11°K$, and $F(T-T_N)\sim3k(T-T_N)/S(S+1)$ [the last relationship requires modification for temperatures very close to T_N], we find that Eq. (6.5) has only one acceptable solution [$\Delta_{eq}=0$] throughout the paramagnetic state. It follows that there is no rhombohedral distortion in the paramagnetic state and that the spin correlation results of Part I may be applied to MnO.

Spin correlations in powder samples of MnO have recently been investigated by Blech and Averbach[37] by means of diffuse neutron scattering measurements. Unfortunately, their results are interpreted by use of a model in which the spin correlations in the paramagnetic state reflect the long-range spin pattern which sets in below T_N. As mentioned above, such a situation would result in a rhombohedral distortion at temperatures above T_N. We have shown that the spin correlations in MnO are likely to depend only on the magnitude of the distance between the spins. In Blech and Averbach's notation, this would result in $|x_i|=1$, $y_i=0$ (see their Table I), and differ from either of the models discussed in Ref. 37.

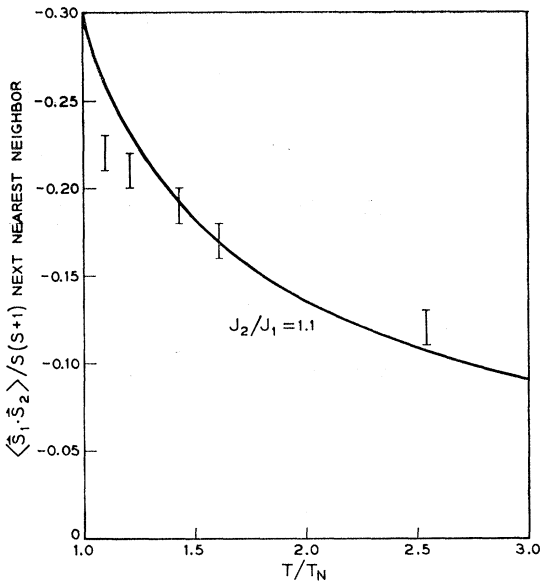

FIG. 15. The next-nearest-neighbor spin correlation curve, as calculated in the random-phase Green's function approximation for $T>T_N$ and for $J_2/J_1=1.1$, is compared with estimates obtained by Blech and Averbach (Ref. 37) from an analysis of diffuse neutron-scattering measurements in MnO.

The results obtained for the even numbered shells, however, would seem to be relatively insensitive to the choice of model, and we might hope that the values obtained for the next-nearest-neighbor spin correlations in Blech and Averbach's[37] Table II are quite good. In Fig. 15 we compare these experimental results with the estimates of the random-phase Green's function theory as given in Part I.

ACKNOWLEDGMENTS

The authors wish to thank R. Lindsay and D. W. Oliver for making available their unpublished results on MnO.